Journal of Sound and Vibration (1998) **212**(5), 875–887

DELAYED-X LMS ALGORITHM: AN EFFICIENT ANC ALGORITHM UTILIZING ROBUSTNESS OF CANCELLATION PATH MODEL

H.-S. KIM AND Y. PARK

Center for Noise and Vibration Control, Department of Mechanical Engineering, Korea Advanced Institute of Science and Technology, Science Town, Taejon 305-701, *Korea*

(*Received* 5 *April* 1995, *and in final form* 5 *January* 1998)

In conventional ANC (Active Noise Control), the cancellation path is usually modelled by a FIR filter with many coefficients. In this study, a Delayed-X LMS algorithm is investigated of which the computational load is much less than that of the Filtered-X LMS method for a long duct or narrow band noise cancellation application. This algorithm is based on the hypothesis that the cancellation path model for the Filtered-X LMS method does not have to be accurate and can be represented by a delay in such cases. The steady state weight vector solution in the presence of model error is investigated to show the validity of using an erroneous simplification. The ADE (Adaptive Delay Estimation) method is proposed for effective delay estimation of the cancellation path, which can be used with the Delayed-X LMS algorithm on-line or off-line. Simulation and experimental results demonstrate the effectiveness of the Delayed-X LMS algorithm for the specified applications.

1. INTRODUCTION

The Filtered-X LMS algorithm [1–3] has been widely investigated and applied as a feed-forward control scheme for ANC (Active Noise Control) systems having an auxiliary path between the control output and the error sensor. When using the Filtered-X LMS, the cancellation path is usually modelled by a FIR filter that has tens of or even hundreds of coefficients in it; filtering the reference signal through the estimated cancellation path model is a heavy burden to real-time controllers. Especially for the MIMO version of Filtered-X LMS, such a computational burden is directly related to the increment of hardware cost.

It must be noted that the approximated cancellation path model can be used without much deterioration in performance. This is the main reason why the cancellation path model obtained off-line, and therefore usually not accurate in a changing environment, can be successfully used in practice. Only if the phase difference between the true cancellation path and the cancellation path model is less than 90° can the stable convergence of the Filtered-X LMS algorithm be guaranteed [4, 5] even though the equilibrium may be different.

In this paper, a Delayed-X LMS algorithm is investigated, in which the cancellation path model is intentionally simplified with only two parameters; delay and gain. Hence, one is considering the case when the cancellation path model is erroneous. It can be viewed as a simplified version of the Filtered-X LMS algorithm utilizing its robustness to the error in the cancellation path's model. Fortunately, such an approximation ensures convergence,

0022–460X/98/200875 + 13 $25.00/0/sv971484

which will be discussed in section 2 for the two applications: ANC for a long duct, and ANC for a narrow band noise. Moreover, it hardly alters the converging value from the optimal as will be seen in section 3 via an analytical investigation and numerical verification. Convergence and performance of the proposed algorithm are discussed for two special applications.

An ADE (Adaptive Delay Estimation) method is proposed, which estimates the delay and gain of the cancellation path model adaptively for the Delayed-X LMS algorithm. This can be used off-line or on-line with small additional computations. Simulation and experimental results show the effectiveness of the proposed method.

A typical block diagram of a single input single output ANC system, which will be considered from now on, is shown in Figure 1. The transfer function $P(z)$, designating the "plant", represents an acoustic system consisting of the system from the reference sensor output to the error microphone output. The "cancellation path" $H(z)$ represents the dynamics from the control output to the error microphone output and $C(z)$ is its model. The reference noise source signal $x(k)$ is measured and filtered through an adaptive filter $W(z)$ in the controller, and drives a control source to cancel the noise. Residual noise $e(k)$ is detected by the error microphone, and is used in the adaptive algorithm (usually LMS-type) to optimize the control performance by minimizing the residual noise itself.

2. DELAYED-X LMS ALGORITHM

2.1. ALGORITHM DESCRIPTION

In feed-forward active noise control when using an FIR-type adaptive filter, the control ouptut $y(k)$ is

$$y(k) = \mathbf{W}^{\mathrm{T}}(k)\mathbf{X}(k), \tag{1}$$

where $\mathbf{W}(k) = [w_0(k)w_1(k) \cdots w_L(k)]^{\mathrm{T}}$ is a column vector of length $L + 1$, whose elements are weights of the adaptive filter $W(z)$ and $\mathbf{X}(k) = [x(k)x(k-1) \cdots x(k-L)]^{\mathrm{T}}$ is a column vector of length $L + 1$ formed by the subsequent reference input signal $x(k)$. The Delayed-X LMS algorithm can be considered as a special type of the Filtered-X LMS in which $gz^{-\Delta}$ is used as a cancellation path model:

$$C(z) = gz^{-\Delta}. \tag{2}$$

Here g and Δ represent the gain and delay of the model, respectively. The main reason for using the simplified model $gz^{-\Delta}$ is its computational benefit. The updated form of the Delayed-X LMS algorithm becomes much simpler than that of Filtered-X LMS,

$$\mathbf{W}(k+1) = \mathbf{W}(k) + 2\eta e(k)g\mathbf{X}(k-\Delta). \tag{3}$$

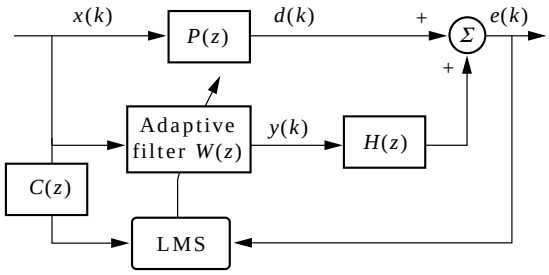

Figure 1. Block diagram of typical ANC system.

In this updated form, the filtered reference signal is replaced by $g\mathbf{X}(k-\Delta)$, no convolution is needed and only accessing delayed data from the memory is necessary. Redefining a new convergence parameter μ that is equal to ηg, one can obtain an alternative and simpler update form:

$$\mathbf{W}(k+1) = \mathbf{W}(k) + 2\mu e(k)\mathbf{X}(k-\Delta). \tag{4}$$

Now, the gain g is not an essential parameter any more; rather the delay Δ and μ are the important parameters.

2.2. ROBUSTNESS OF CANCELLATION PATH MODEL—NUMERICAL SIMULATION

The existence of stable bounds for various delays in the Delayed-X LMS algorithm will be illustrated. The upper stable bound of μ, denoted as μ_s, is directly found from updating the Delayed-X LMS algorithm by trial and error in the simulation.

For simulation, two tone signals with 200 and 300 Hz (under 2 kHz sampling) and peak to peak magnitude of unity were used as the reference signal $x(k)$. The weight length $\mathbf{W}$ was 5. The upper stable bound μ_s is plotted in Figure 2 versus Δ ($\Delta = 0, 1, 2, \ldots, 10$), which represents the delay of the cancellation path model. The plant is set as $P(z) = 0{\cdot}3z^{-6} + z^{-7} + 2z^{-8} + z^{-9} + 0{\cdot}1z^{-10}$, and the following three cases of $\mathbf{H}$ (the vector formed by impulse response of $H(z)$) are considered:

$$\mathbf{H} = \begin{Bmatrix} [0 & 1 & 2 & 3 & 4 & 5 & 4 & 3 & 2 & 1 & 0]^{\mathrm{T}}, & \text{Case I} \\ [0 & 1 & 2 & 3 & 4 & 0 & -4 & -3 & -2 & -1 & 0]^{\mathrm{T}}, & \text{Case II} \\ [0 & 1 & 2 & 3 & 4 & 3 & 2 & 1 & 0 & -1 & 0]^{\mathrm{T}}, & \text{Case III} \end{Bmatrix}.$$

While $\mathbf{H}$ of Case I or II is a linear phase system, that of Case III is not. As shown in Figure 2 there are many simply delay models that ensure convergence for all three cases of $\mathbf{H}$. The μ_s for Case I is almost symmetric as is $\mathbf{H}$. The shape of μ_s for the Cases II and III have peaks at the same related position of $\mathbf{H}$.

The existence condition of a stable μ mainly depends on the phase difference between $\mathbf{H}$ and its model. A non-zero μ_s implies that the phase error between $\mathbf{H}$ and its model is less than 90° for both 200 and 300 Hz, which is easy to prove analytically from the previous $\mathbf{H}$ and its simplified model. This was confirmed for the three cases of $\mathbf{H}$. Also, one could observe that there are many possible delay models that can show stable convergence for the three cases considered.

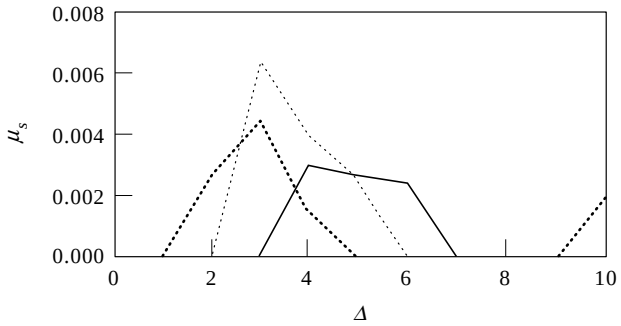

Figure 2. Upper stable bound μ_s versus Δ for three cases of $H(z)$ when reference is a two-tone signal (200 and 300 Hz reference under 2 kHz sampling). ——, Case I; - - - -, Case II; · · · ·, Case III.

3. EFFECTS OF MODEL ERROR OF C AT STEADY STATE

3.1. STEADY STATE SOLUTION

In this section, an investigation is made of how the error in the model of the cancellation path affects the steady state weight vector $\mathbf{W}^*$, and which condition leads $\mathbf{W}^*$ to its ideal optimum value $\mathbf{W}^*_{opt}$ that can be obtained from an error-free $C(z)$. The error surface $e(k)^2$ is of a quadratic form with respect to $\mathbf{W}$ and the minimum is independent of $C(z)$. *However, since its calculation of the gradient is distorted, when $C(z)$ is erroneous, it may lead W to a steady state* $\mathbf{W}^*$ *that is not the global minimum* $\mathbf{W}^*_{opt}$. At first though one might conclude that this fact weighs against adopting a simplified cancellation path model. But the investigation of the steady state solution in detail reveals that error in $C(z)$ does not degrade the performance in some important cases.

One can rearrange the Filtered-X LMS update equation at steady state as

$$\mathcal{C}^{\mathrm{T}}\mathbf{R}\mathcal{H}\mathbf{W}^* = -\mathcal{C}^{\mathrm{T}}\mathbf{R}\mathbf{P}, \tag{5}$$

where

$$\mathcal{C} = \underbrace{\begin{bmatrix} \mathbf{C} & & \mathbf{0} \\ & \mathbf{C} & \\ & \ddots & \\ \mathbf{0} & & \mathbf{C} \end{bmatrix}}_{(L+M+1)\times(L+1)}, \qquad \mathbf{C} = [c_0 \cdots c_M]^{\mathrm{T}}, \tag{6}$$

$$\mathcal{H} = \underbrace{\begin{bmatrix} \mathbf{H} & & \mathbf{0} \\ & \mathbf{H} & \\ & \ddots & \\ \mathbf{0} & & \mathbf{H} \end{bmatrix}}_{(L+M+1)\times(L+1)}, \qquad \mathbf{H} = [h_0 \cdots h_M]^{\mathrm{T}}, \tag{7}$$

$$\mathbf{R} = \mathbf{E}[[x(k)\cdots x(k-L-M)]^{\mathrm{T}}[x(k)\cdots x(k-L-M)]], \qquad \mathbf{P} = [p_0 \cdots p_{L+M}]^{\mathrm{T}}. \tag{8, 9}$$

Here, $\mathbf{C}$, $\mathbf{H}$ and $\mathbf{P}$ are vectors formed from the coefficients of $C(z)$, $H(z)$ and $P(z)$, respectively. Letting $\mathbf{W}_0$ be the weight's initial value, one can write $\mathbf{W}^*_{opt}$ and the steady state value $\mathbf{W}^*$ as

$$\mathbf{W}^*_{opt} = -(\mathcal{H}^{\mathrm{T}}\mathbf{R}\mathcal{H})^{+}\mathcal{H}^{\mathrm{T}}\mathbf{R}\mathbf{P} + [\mathbf{I} - (\mathcal{H}^{\mathrm{T}}\mathbf{R}\mathcal{H})^{+}(\mathcal{H}^{\mathrm{T}}\mathbf{R}\mathcal{H})]\mathbf{W}_0, \tag{10}$$

$$\mathbf{W}^* = -(\mathcal{C}^{\mathrm{T}}\mathbf{R}\mathcal{H})^{+}\mathcal{C}^{\mathrm{T}}\mathbf{R}\mathbf{P} + [\mathbf{I} - (\mathcal{C}^{\mathrm{T}}\mathbf{R}\mathcal{H})^{+}(\mathcal{C}^{\mathrm{T}}\mathbf{R}\mathcal{H})]\mathbf{W}_0, \tag{11}$$

where the superscript $+$ denotes the pseudo-inverse.

Equation (11) can be categorized and simplified into three cases according to the condition of the noise spectra. Suppose the reference $x(k)$ is composed of N distinct frequency components. The rank of $\mathcal{C}^{\mathrm{T}}\mathbf{R}\mathcal{H}$ is $\min\{2N, L+1\}$ because the rank of $\mathbf{R}$ is $\min\{2N, L+M+1\}$ and the rank of $\mathcal{C}$ and $\mathcal{H}$ are all $L+1$. One can categorize the noise property into three cases: $2N$ is less than $L+1$ (under-determined case); $2N$ is greater than $L+1$ (over-determined case); $2N$ is equal to $L+1$ (non-singular case). Such a categorization is based on the fact that each frequency component needs two coefficients

to be suppressed. One can rewrite equation (11) for the successive three cases as follows:

$$\mathbf{W}^* = (\mathbf{RH})^+\mathbf{RP} + [\mathbf{I} - (\mathbf{RH})^+(\mathbf{RH})]\mathbf{W}_0, \qquad \text{under-determined case;} \tag{12}$$

$$\mathbf{W}^* = -(\mathbf{C}^{\mathrm{T}}\mathbf{RH})^{-1}\mathbf{C}^{\mathrm{T}}\mathbf{RP}, \qquad \text{over-determined case;} \tag{13}$$

$$\mathbf{W}^* = -(\mathbf{RH})^+\mathbf{RP}, \qquad \text{non-singular case.} \tag{14}$$

For the under-determined case (equation (12)), $\mathbf{W}^*$ is independent of $C(z)$, but it depends on the initial weight $\mathbf{W}_0$. For the over-determined case (equation (13)), $\mathbf{W}^*$ depends on $C(z)$ and is independent of $\mathbf{W}_0$, which is the opposite to that of the under-determined case. For the non-singular case (equation (14)), $\mathbf{W}^*$ is independent of both $C(z)$ and $\mathbf{W}_0$.

The first and second terms, of the right side of equation (12) are orthogonal to each other and the second term can be controlled by $\mathbf{W}_0$. Because the initial weight $\mathbf{W}_0$ can be chosen arbitrarily, there is an infinite number of acceptable $\mathbf{W}^*$ for the under-determined case. Among the numerous solutions, the best one will be the one that requires minimum power, which can be obtained by setting $\mathbf{W}_0$ to be the zero vector. One must start to update the weight after full development of the filtered-x signal to see the effect of $\mathbf{W}_0$ without distortion, because adaptation of $\mathbf{W}$ at the initial state could be distorted by the time-varying filtered-x signal that is not fully developed.

Note that *for under-determined and non-singular cases*, $\mathbf{W}^*$ *equals* $\mathbf{W}^*_{opt}$ *even though* $\mathbf{C}$ *is different from* $\mathbf{H}$. Thus, for narrow band noise suppression, $C(z)$ is a dummy in respect to the steady state value providing that the length of $\mathbf{W}$ is sufficiently long and convergence is achieved.

3.2. EXAMPLES OF STEADY STATE SOLUTION

The reference input is composed of two pure tones of 200 and 700 Hz with the same peak to peak magnitude of unity. The plant and cancellation path are chosen as the FIR filter model as follows: $P(z) = 0{\cdot}3z^{-5} + z^{-6} + 2z^{-7} + z^{-8} + 0{\cdot}1z^{-9}$, $H(z) = 0{\cdot}2z^{-4} + z^{-5} + 0{\cdot}1z^{-6}$ for a 2 kHz sampling frequency. Two cases of $C(z)$ are considered, exact modelling and erroneous modelling, and two cases of $\mathbf{W}_0$, zero initial values and non-zero initial values. Thus, four cases were simulated as follows:

$C(z)$	$\mathbf{W}_0 = [0 \quad 0 \quad 0 \quad \cdots]^{\mathrm{T}}$ (zero initial $\mathbf{W}_0$)	$\mathbf{W}_0 = [-0{\cdot}3 \quad 0{\cdot}3 \quad -0{\cdot}3 \quad \cdots]^{\mathrm{T}}$ (non-zero initial $\mathbf{W}_0$)
$C(z) = H(z)$ (no error in $\mathbf{C}$)	Case 1	Case 2
$C(z) = H(z) - 0{\cdot}1z^{-6}$ (error in $\mathbf{C}$)	Case 3	Case 4

Two different weight lengths of 10 and 3 were considered, which represent the under-determined and over-determined cases, respectively. The Filtered-X LMS algorithm was adapted until the steady state was reached, and the resultant weight with the $\mathbf{W}^*$ obtained from the analytical solution is shown in Figures 3(a) and 4(a). The FRF (Frequency Response Function) of $\mathbf{W}^*$ and its target transfer function $-P(z)/H(z)$, are shown in Figures 3(b) and 4(b). The analytical solutions were identical to the steady state weights of the Filtered-X LMS within the drawing resolution of the graph. In the under-determined case, as shown in Figure 3, $C(z)$ could not change the $\mathbf{W}^*$ (since the results of Cases 1 and 3 are equal and the results of Cases 2 and 4 are equal), whereas the effect of $\mathbf{W}_0$ remains throughout the adaptation as shown in the FRF. However, at 200 and 700 Hz all the three results ((i) $-P/H$, (ii) analytical solution, and (iii) steady state value of Filtered-X LMS) have the same magnitudes and phases. In the

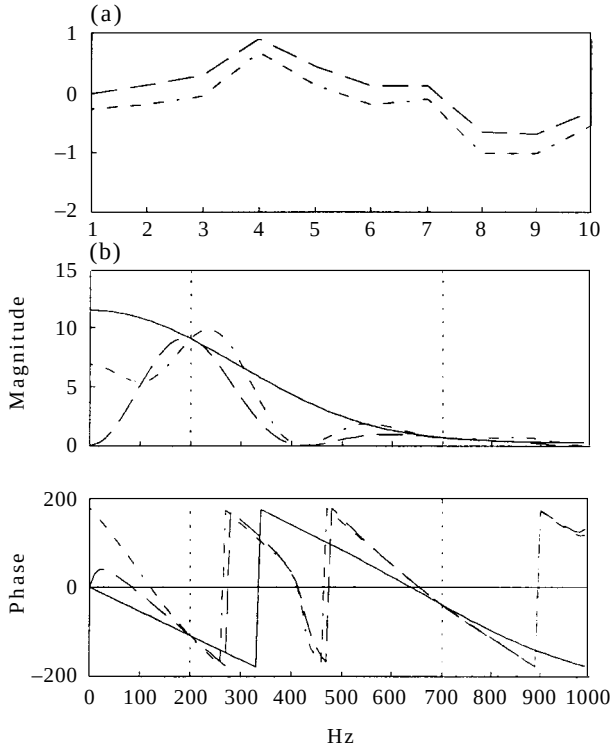

Figure 3. **W*** of under-determined case (filter length 10, 200 Hz and 700 Hz noise): (a) **W*** shape; (b) FRF of **W***. ——, $-P/H$; – – –, Cases 1 and 3; -----, Cases 2 and 4.

over-determined case, as shown in Figure 4, $\mathbf{W}_0$ does not affect the steady solution as the results of Cases 1 and 2 are equal and the results of Cases 3 and 4 are equal. A different cancellation path model leads **W*** to a different shape. Note that the magnitude and phase at 200 and 700 Hz cannot be matched because of the lack of degree of freedom in the weight vector **W**.

4. ESTIMATION OF CANCELLATION PATH MODEL FOR DELAYED-X LMS

4.1. ADAPTIVE DELAY ESTIMATION (ADE)

The cancellation path (a) in a long duct system (each end is well treated with absorbing material) or (b) for narrow band noise can be approximately modelled as a time delay system with a gain as in equation (2). The purpose of the ADE method is to adapt the Δ required in the Delayed-X LMS algorithm of equation (4). Off-line identification is the most convenient way to identify the cancellation path's delay if modelling of $H(z)$ is available *a priori*. The maximum absolute peak position of the impulse response of $H(z)$ is a proper choice for the delay Δ and the peak value is a proper choice of the gain g. To get Δ adaptively in real time, one could identify $H(z)$ with the FIR model and determine Δ from the impulse response as one does in off-line. This idea will suffice. However, it is advantageous to use the ADE algorithm that can directly adapt Δ to reduce computation and programming complexity.

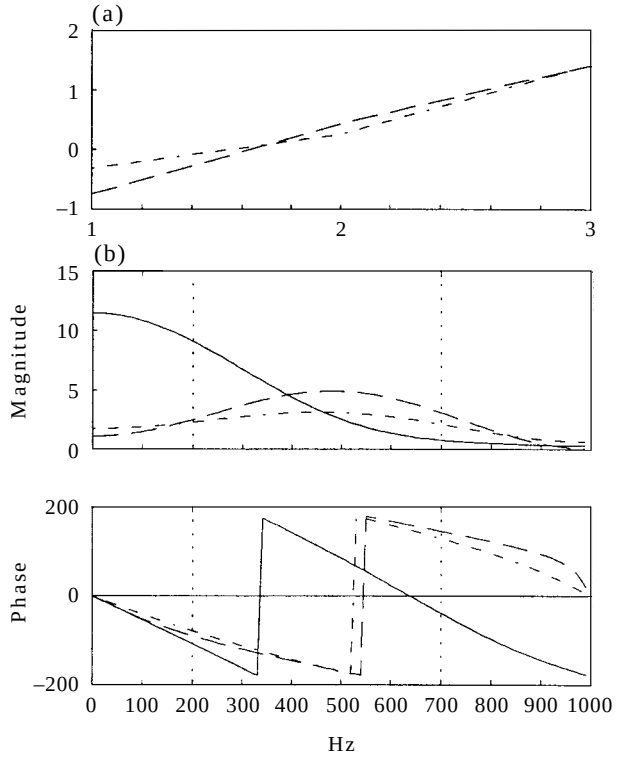

Figure 4. **W*** of over-determined case (filter length 3, 200 Hz and 700 Hz noise): (a) **W*** shape; (b) FRF of **W***. ——, $-P/H$; — — —, Cases 1 and 2; ----, Cases 3 and 4.

The control source input $y(k)$ is not orthogonal to $e(k)$ at the initial stage, in general. One can utilize the information of $H(z)$ left in $e(k)$ at the initial stage of adaptation for achieving Δ. Suppose $d(k)$ due to the primary noise source is a disturbing noise (in the sense of adapting Δ), and define the cost function as

$$J(k) = s(k)^2, \tag{15}$$

where

$$s(k) = e(k) - \hat{e}(k) = d(k) + H(z)y(k) - y(k - \Delta(k)). \tag{16}$$

Figure 5 is schematic diagram of the ADE part. It has an LMS structure where $y(k)$ is the input and $s(k)$ is the error quantity. Using the steepest descent method to minimize the cost function one can update g and Δ as

$$g(k+1) = g(k) - 2\mu_g \nabla_g(k), \qquad \Delta(k+1) = \Delta(k) - 2\mu_\Delta \nabla_\Delta(k), \tag{17, 18}$$

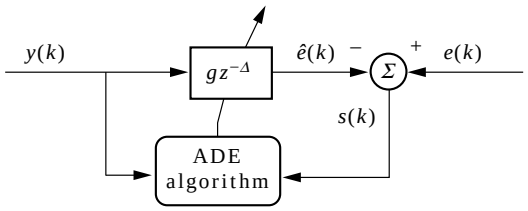

Figure 5. Block diagram of ADE.

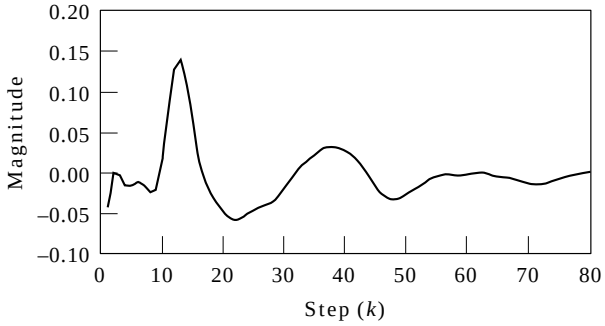

Figure 6. Impulse response of cancellation path of a long duct system (2·5 kHz sampling).

where $\nabla_g(k)$ and $\nabla_\Delta(k)$ are the gradients of $s(k)^2$ with respect to g and Δ, respectively, and μ_g and μ_Δ are convergence parameters. From equations (17) and (18), one finds

$$g(k+1) = g(k) + 2\mu_g s(k) y(k - \text{round}(\Delta(k))), \tag{19}$$

$$\Delta(k+1) = \Delta(k) + 2\mu_\Delta s(k) g(k)\{y(k - \text{round}(\Delta(k)) + 1) - y(k - \text{round}(\Delta(k)) - 1)\}. \tag{20}$$

The $\Delta(k)$ must be rounded to the nearest integer to be used as a time-step delay. The central difference method is used to get $\nabla_\Delta(k)$. Of course, either the backward or forward difference method is possible to get $\nabla_\Delta(k)$.

The error surface $s(k)^2$ with respect to g and Δ is a function of the noise spectrum of the excitation signal. Two error surfaces for a 50–400 Hz band signal and for a 300 Hz single tone signal for the cancellation path $H(z)$ (of Figure 6 obtained from a long duct system), are shown in Figures 7(a) and (b), respectively. Note that the error surface is deformed by the stochastic characteristics of the excitation signal. The optimal position is periodically located for the tonal signal, because any Δ which is of an integer multiple

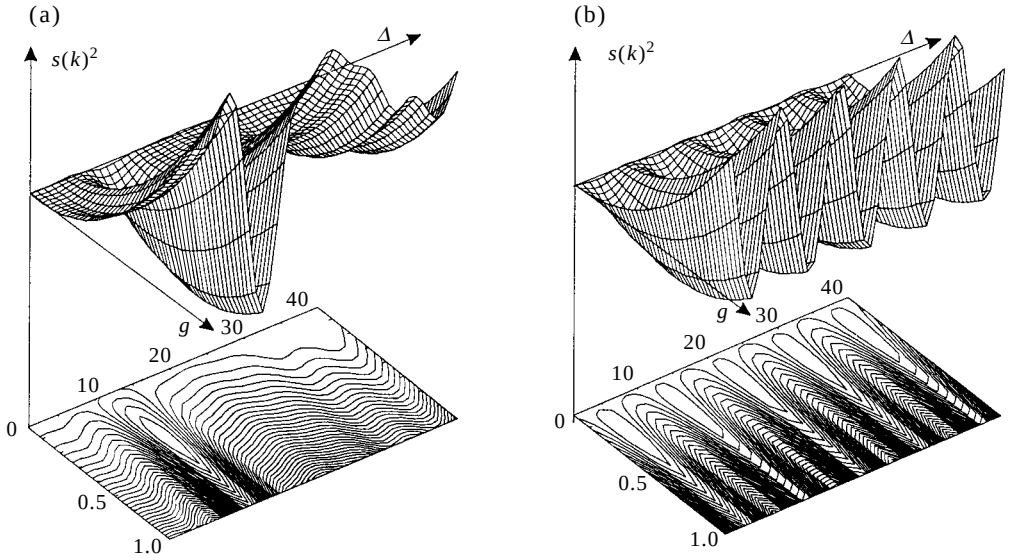

Figure 7. Error surfaces of the cancellation path of Figure 6 with simplified model $gz^{-\Delta}$: (a) for 50–400 Hz band signal; (b) for 300 Hz pure tone signal.

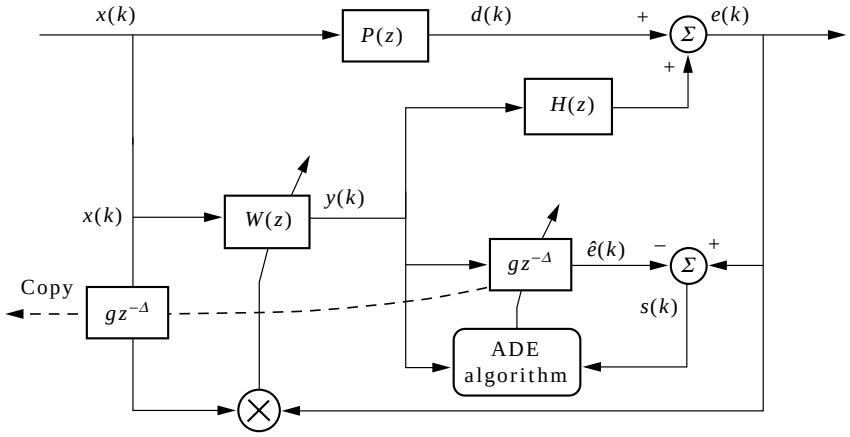

Figure 8. Block diagram of Delayed-X LMS with on-line ADE.

of the period minimizes $s(k)^2$. Also note that the gradient is not affected by the gain g, but the initial guess of Δ is critical to the convergence to the global minimum. The following formula is recommended for the initial guess of Δ:

$$\Delta = l/(cT_s) + D/T_s, \tag{21}$$

where l is the shortest length of the cancellation path (m), c is the speed of sound (m/s), D is a combined time delay of electrical parts in the cancellation path (s), and T_s is the sampling time (s/step).

4.2. DELAYED-X LMS WITH ADE

ADE can be used with Delayed-X LMS either on-line or off-line. Delayed-X LMS with on-line ADE gives computational advantage over the conventional on-line methods [6, 7] by using a simplified model for the cancellation path instead of the full FIR model. Providing that all the filter lengths are equal, the computational load is 67% of the conventional method. If on-line ADE is used, the computational load is only 40% of the conventional on-line cancellation path detection scheme.

Figure 8 is the schematic diagram of Delayed-X LMS with on-line ADE. At each adaptation step, the weight vector, the estimated gain, and the delay of the cancellation

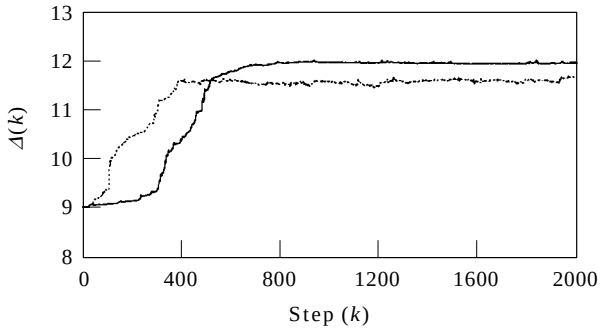

Figure 9. On-line (· · · ·) and off-line (——) ADE estimation of Δ.

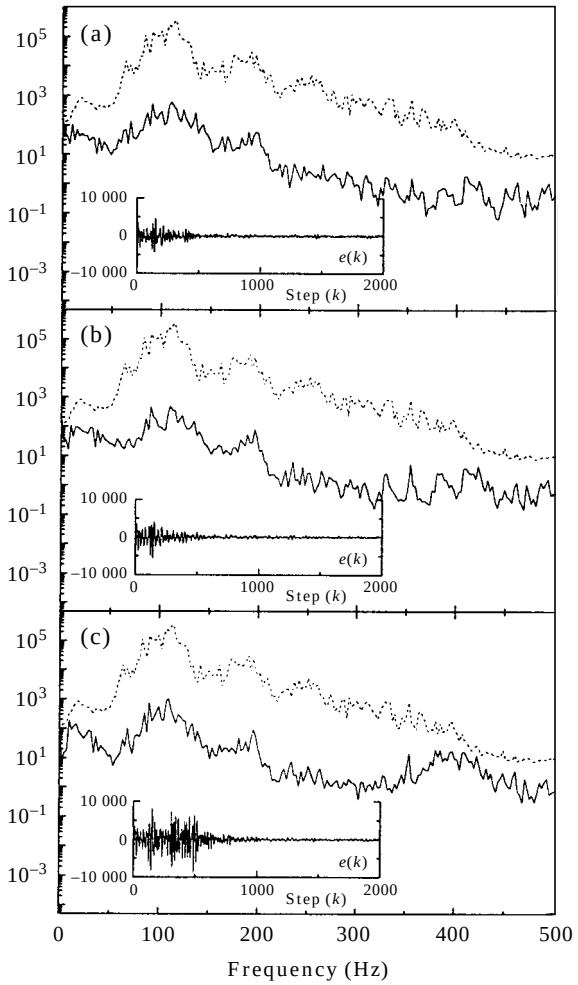

Figure 10. Simulation results for a long duct system: (a) Filtered-X LMS; (b) Delayed-X LMS with off-line ADE; (c) Delayed-X LMS with on-line ADE. · · · · ·, Before ANC; ——, after ANC.

path are updated simultaneously by using equations (4), (19) and (20). A fixed g instead of $g(k)$ is recommended for filtering the reference signal, because $g(k)$ goes to zero as the $d(k)$ signal is cancelled by $H(z)y(k)$ and the information of the cancellation path disappears in $e(k)$. However, the drift of Δ at steady state can be drastically reduced by using the $g(k)$ term in its gradient part. One can use a parallel on-line cancellation path modelling method [7] with a simplified cancellation path and plant models to reduce such contamination phenomena. Proper adjustment of μ, μ_g, and μ_Δ is recommended to ensure relatively faster convergence of g and Δ than that of $\mathbf{W}$.

5. COMPUTER SIMULATION AND EXPERIMENTAL RESULTS

5.1. SIMULATION RESULT

The data measured from a real duct system was used to get more realistic results in the simulation. For a long duct system, a finite duct was used both ends of which were treated by absorptive material to avoid reflection at the frequency of interest. The data and the

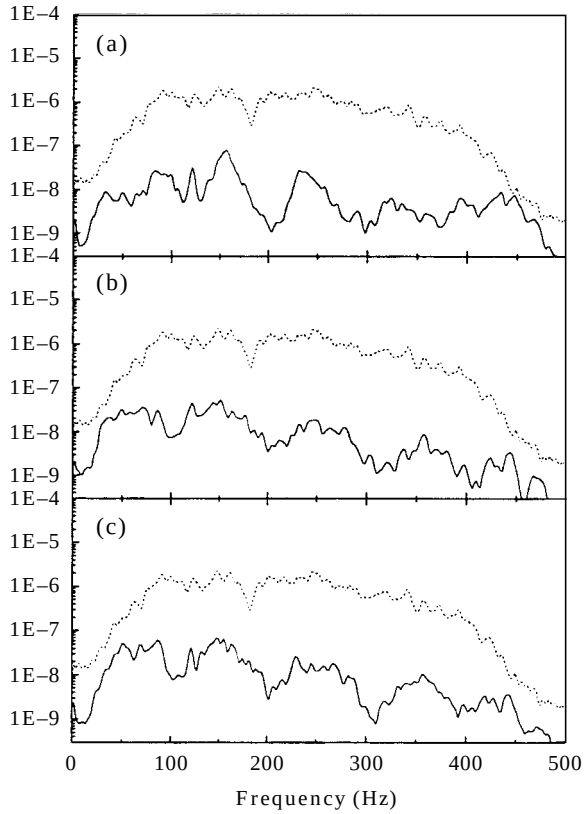

Figure 11. Experimental result for a long duct system: (a) Filtered-X LMS; (b) Delayed-X LMS with off-line ADE; (c) Delayed-X LMS with on-line ADE. Key as Figure 10.

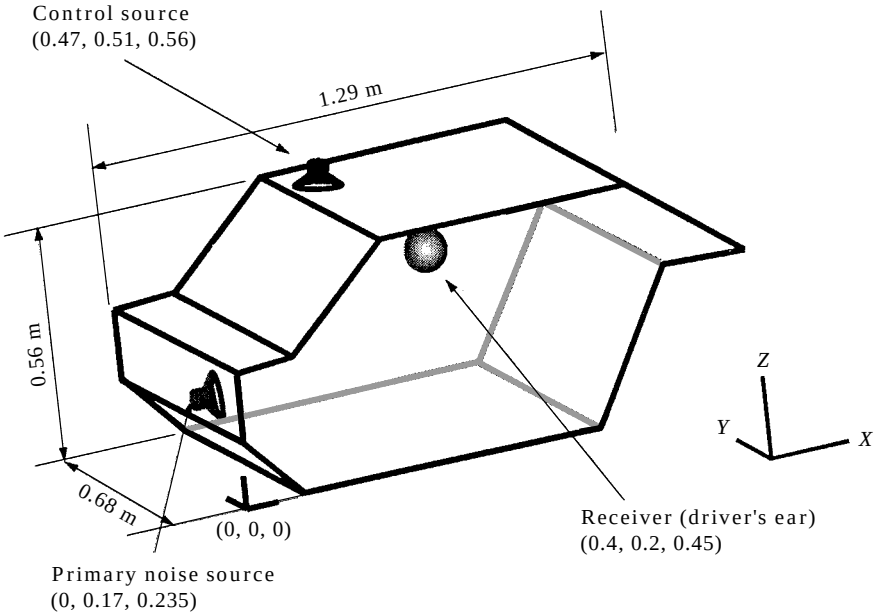

Figure 12. Experimental set-up for ANC of narrow band noise in a half scale car cabin.

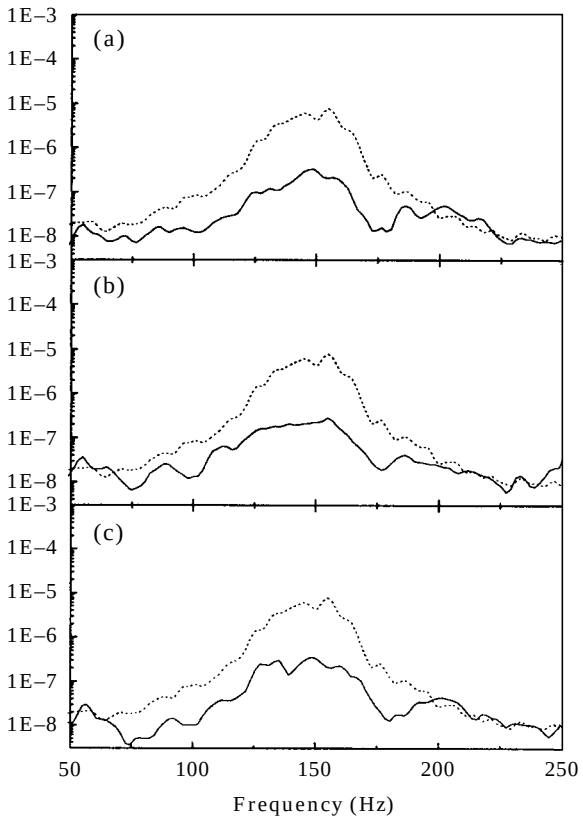

Figure 13. Experimental result for a narrow band noise in a half scale car cabin: (a) Filtered-X LMS; (b) Delayed-X LMS with off-line ADE; (c) Delayed-X LMS with on-line ADE. Key as Figure 10.

cancellation path $H(z)$ for the simulation were obtained from a duct system with a 2500 Hz sampling rate. By exciting $H(z)$ with a random signal whose frequency range is of 50–400 Hz band, the model of the cancellation path $H(z)$ was obtained by LMS adaptation with 80 coefficients. Figure 6 shows the cancellation path model obtained from the experiment. It is assumed to be the actual cancellation path $H(z)$. The plant $P(z)$ was set to $H(z)^2$ for convenience. Figure 9 is the plot of the off-line and on-line estimation of Δ for the given $H(z)$. One can observe that the two curves of round(Δ) converge to the global minimum position (round(Δ) = 12) of the error surface in Figure 7(a). A faster convergence speed is achieved for on-line ADE because the initial magnification of the signal $y(k)$ followed by a wrong adaptation of $\mathbf{W}$ results in the enlargement of the excitation signal and speeds up the update of the delay.

Figure 10 shows the performance comparison of the three algorithms: (a) the conventional Filtered-X LMS; (b) Delayed-X LMS with off-line ADE; (c) Delayed-X LMS with on-line ADE. Each power spectrum was drawn averaging data of $2000 \leqslant k \leqslant 5500$. The noise reduction achieved by the Delayed-X LMS algorithm is not worse than that achieved by the Filtered-X LMS, though its computational load is reduced significantly. Delayed-X LMS with on-line ADE takes more time to converge because the initial guess of Δ is different from the optimal one. It takes about 500 steps for Δ to converge, as shown in Figure 9.

5.2. EXPERIMENTAL RESULT

The feasibility of Delayed-X LMS in the two applications (ANC for a long duct system and for a narrow band noise) was verified by experiments. For the experiments, a TMS320c40 DSP board in connection with a notebook computer was used with a 2 kHz sampling rate.

A circular duct of 15 cm diameter with a control source at a distance of 195 cm from a primary source, and an error microphone at a distance of 102 cm from the control source were used. A reference noise whose band is 100–400 Hz was generated by a random signal generator and was fed to the primary source. FIR filters with a filter length of 84 were used for $W(z)$ and $C(z)$. Figure 11 shows the steady state power spectrum of the error microphone signal before and after the real-time control for a long duct system with an average of 20 data sets.

Figure 12 shows an experimental set-up in which a primary, a control source and an error microphone were located in a half scale car cabin model. A narrow band noise with a band width of 31·6 Hz and a center frequency of 150 Hz obtained from the random signal generator was supplied to the primary source. The adaptive filter $W(z)$ and the cancellation path model $C(z)$ with a filter length of 32 were used in this case. Figure 13 shows the experimental results of ANC for this narrow band noise application.

Similar to the simulation results, the experimental results show that the performance of the Delayed-X LMS with on-line or off-line ADE almost matches that of Filtered-X LMS.

6. CONCLUSIONS

The use of a Delayed-X LMS algorithm has been investigated for a system where, though the cancellation path is not exactly a delaying system, intentional simplification of the cancellation path model is possible. The Delayed-X LMS algorithm is advantageous in computational time and memory requirement because of the elimination of the convolution operation required in the conventional Filtered-X LMS method. The validity of using the proposed algorithm has been shown for ANC of a long duct system or narrow band noise suppression applications where erroneous modelling does not degrade the steady state performance. To obtain the delay of the cancellation path efficiently an ADE method has been proposed that can be used off-line or on-line. The effectiveness of the Delayed-X LMS algorithm with ADE was demonstrated through simulations and experiments.

REFERENCES

1. B. Widrow and S. D. Stearns 1985 *Adaptive Signal Processing*. Englewood Cliffs, NJ: Prentice-Hall. Inc.
2. J. C. Burgess 1981 *Journal of the Acoustical Society of America* **70**, 715–726. Active adaptive sound control in a duct: a computer simulation.
3. L. A. Poole, G. E. Warnaka and R. C. Cutter 1984 *IEEE International Conference on Acoustics*, *Speech*, *and Signal Processing*, 21.7–21.7.4. The implementation of digital filters using a modified Widrow–Hoff algorithm for the adaptive cancellation of acoustic noise.
4. S. D. Snyder and C. H. Hansen 1990 *Journal of Sound and Vibration* **141**, 409–424. The influence of transducer transfer functions and acoustic time delays on the implementation of the LMS algorithm in active noise control system.
5. D. R. Morgan 1980 *IEEE Transactions on Acoustics*, *Speech*, *and Signal Processing* **28**, 454–467. An analysis of multiple correlation cancellation loops with a filter in auxiliary path.
6. L. J. Eriksson 1989 *Journal of the Acoustical Society of America* **85**, 797–802. Use of random noise for on-line transducer modeling in an adaptive active attenuation system.
7. S. M. Kuo, M. Wang and K. Chen 1992 *Noise Control Engineering Journal* **39**, 119–171. Active noise control system with parallel on-line error path modeling algorithm.